Energy 141 (2017) 624–634

Contents lists available at ScienceDirect

Energy

journal homepage: www.elsevier.com/locate/energy

Wave energy trends over the Bay of Biscay and the consequences for wave energy converters

Alain Ulazia [a, *], Markel Penalba [c], Gabriel Ibarra-Berastegui [e, b], John Ringwood [c], Jon Saénz [d, e]

[a] Department of NE and Fluid Mechanics, University of the Basque Country (UPV/EHU), Otaola 29, 20600 Eibar, Spain
[b] Department of NE and Fluid Mechanics, University of the Basque Country (UPV/EHU), Alda. Urkijo, 48013 Bilbao, Spain
[c] Centre for Ocean Energy Research, Maynooth University. Maynooth, Co, Kildare, Ireland
[d] Department of Applied Physics II, University of the Basque Country (UPV/EHU), B. Sarriena S/n, 48940 Leioa, Spain
[e] Joint Research Unit (UPV/EHU-IEO) Plentziako Itsas Estazioa, University of Basque Country (UPV/EHU), Areatza Hiribidea 47, 48620 Plentzia, Spain

ARTICLE INFO

Article history:
Received 5 July 2017
Received in revised form
20 September 2017
Accepted 21 September 2017
Available online 23 September 2017

Keywords:
Wave energy trends
ERA-Interim
ERA-20C
Wave energy converters
Fluid mechanics

ABSTRACT

This is one of the pioneer and preliminary attempt to study the influence of wave energy trends on the absorbed power of wave energy converters. For that purpose, the reanalysis of the past century ERA20 has been calibrated via quantile-matching against the reanalysis ERA-Interim in their intersection period (1979–2010). The validation against four buoys in the Bay of Biscay is presented in this paper, showing a better agreement of ERA-Interim-WAM model when compared to the original ERA20. In addition, calibrated ERA20 shows a significant error reduction compared to the original ERA20. Hence, calibrated ERA20 presents an increment of the wave energy resource, more than 1 kW/m per decade, in the area of study and a general increment of the wave height and wave period throughout the analyzed decades. Finally, using the calibrated series at a given gridpoint in the bay, power absorption of a generic wave energy converter (WEC) is examined, combining the power matrix of the WEC and the two-variable (wave height and period) probability density functions (PDF) of the five do-decades of the past century. Results show important variations of the PDF, which results in significant differences, up to a 15% increase between two do-decades, in the annual mean power production.

1. Introduction

The interest in wave energy has increased significantly in the last decades due to the need for clean energy sources to reduce the increasing greenhouse emissions. Although none of the wave energy converters (WECs) has reached the commercial stage yet, wave energy is expected to contribute to the future energy supply system. The Mutriku Wave Energy Plant is based on the oscillating water column principle to absorb wave power from ocean waves and is one of the very few existing wave power plants connected to the electricity grid [1].

Accurate characterization of the wave energy resource is essential to appropriately design the wave energy plants of the future. In general, wave data from previous years is employed to determine the potential of a specific location [2] and estimate absorbed energy and power of a specific WEC [3]. Considering only wave data from previous years, variations of the resource over longer time periods, i.e. decades, cannot be taken into account, meaning that the data used to design the wave energy plant and the real resource the WEC extracts energy from, may be significantly different. In order to make reliable estimations of the distribution of climate variables, the World Meteorological Organization [4,5] proposes the use of 30 years of data.

Therefore, studying variation trends of the wave energy resource is crucial for an accurate resource characterization and power production assessment. However, the different studies about wave trends presented in the literature to date and to the best knowledge of the authors, have been focused mainly on the variation of the wave height. These studies on wave trends typically use data from four different sources:

1. In situ measurements by buoys [6],

* Corresponding author.
E-mail addresses: alain.ulazia@ehu.eus (A. Ulazia), mpenalba@eeng.nuim.ie (M. Penalba), gabriel.ibarra@ehu.eus (G. Ibarra-Berastegui), john.ringwood@eeng.nuim.ie (J. Ringwood), jon.saenz@ehu.eus (J. Saénz).

https://doi.org/10.1016/j.energy.2017.09.099
0360-5442/

2. Wave observations from ships [7–10],
3. Satellite altimeter [11,12],
4. And model and reanalysis datasets [13–22].

With respect to the last case, models and reanalysis, one of the closest studies to the present paper is the global study on wave energy resources by Zheng eta al [15]. They use the 40-year reanalysis ERA40, previous to ERA-Interim-WAM, and present an integral study on wave energy focused on many different aspects, calculating wave trends via lineal regression instead of the Theil-Sen method over monthly anomalies (see Section 2.2) used in the present paper. The same author has recently presented another global study [13] using a completely different method based on the swell index and the propagation characteristics of swell energy. However, since [13] is a global study focused on climate patterns, results for the Bay of Biscay are not relevant, similarly to Reguero's previous study [14], because the relationships between wave energy flux and the Arctic Oscillation (AO), the PacificNorth America (PNA) index, the North Atlantic Oscillation (NAO), and the East PacificNorth Pacific (EPNP) pattern show low correlations in the interior of the Bay.

Likewise, Bertin et al. [16] have also used the ERA20C reanalysis over the North Atlantic Ocean for the estimation of the wave height trend, and its relationship with the increase of wind speed. They have found a linear positive trend between 0.05 m/decade and 0.025 m/decade around the Bay of Biscay, which is consistent with the results shown in the present paper (see 3). However, in Ref. [16], pure wave height ERA20C data (without calibration) are used and the main focus of the study is the relationship between wave trends and climatic change, instead of wave energy flux.

With regards to remote sensing data, the precision of satellite altimetry has considerably improved in the previous years, generating highly interesting data for long-term wave trend estimation. For instance [12], constitutes a study of wind speed and wave height trends in a global scale. In fact, is the only analysis since 2010 that covers the same area of study as in this paper (the Bay of Biscay). However, it only covers a period of 23 years (1985–2008), which may be insufficient to draw strong conclusions of the wave trends [12]. shows no significant statistical trend for wave height analyzing mean monthly values. At more extreme conditions (90% percentile), there is a clear trend of increasing wave height at high latitudes and more neutral conditions in equatorial regions. According to [12], in the Bay of Biscay the trends are generally neutral, with a weak positive trend between 0 and 0.25% per year in the southeastern part of the Bay, that is, up to 5 cm increase per decade considering a typical 2 m mean wave height [12], Fig. 1].

However, the cycle of the satellites lasts tens of days. Therefore, the temporal resolution of satellite altimetry is not appropriate for high temporal resolution studies [23], which suggests that in situ buoy measurements and ship observations are better candidates. In the southern Bay of Biscay, most important in situ wave data are given by the buoys of the Spanish Port Authority [24] and ship data collected by Gulev et al. in the last decade [7–9].

As an extreme case with in situ observations near the Bay of Biscay, Bouws [10] used historical hand-drawn wave charts of the south of England, at the Seven Stones Corner Light Vessel, and demonstrated a positive trend in wave height of 24 cm/decade over the period 1960–1985. Gulev et al. [7–9] used centennial time series of a visually observed wave data set along the major ship routes in the world, demonstrating positive trends in significant wave height (H_s) of up to 12–14 cm/decade in the North Atlantic around Newfoundland. Gulev's colored map for Europe indicates a trend of 4–6 cm/decade in the interior of the Bay of Biscay and higher trends over the border of the Bay and towards the open Atlantic Ocean (*ibid.*).

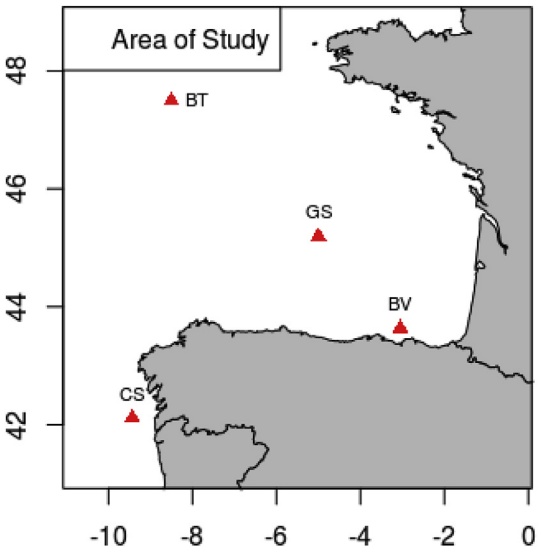

Fig. 1. The area of study and the four buoys.

Variations in wave height are reasonably well documented at different locations all over the world. However, to the best knowledge of the authors, no study in the literature has examined the trends of wave periods related to wave energy production. For example, recently, Camus et al. [25] and Patra et al. [26] have analyzed wave period trends, but in the context of future projections and coastal impact assessment or climate variability. These type of works are recent because until 2005 satellite and remote sensing observations on wave period was considered unreliable [27]. Therefore, the work presented in this paper is the first complete study on historical wave power trends and its influence on the performance of WECs using 20th century data from reanalysis.

The remainder of the paper is as follows: Section 2 describes the data sets, the methodology employed for the evaluation of the wave trend and the hydrodynamic model of the WEC, Section 3 shows the wave trends and the influence of these wave trends on WECs, Section 4 develops the discussion about various aspects, and Section 5 presents the conclusions and the future outlook.

2. Data and methodology

2.1. Data

2.1.1. ERA-20C and ERA-Interim

The global atmospheric data sets used in this work are two reanalysis of the European Centre for Medium-Range Weather Forecasts (ECMWF):

- ERA-20C (henceforth ERA20) [28]. This reanalysis is ECMWF's first atmospheric reanalysis of the 20th century, from 1900 to 2010. ERA20 assimilates observations of surface pressure and surface marine winds from ISPDv3.2.6 and ICOADSv2.5.1 [29] by means of a 24-h 4D-Var analysis method in combination with a coupled atmosphere/land-surface/ocean-waves model. The horizontal resolution is approximately 125 km and wave parameters can be obtained 3-hourly. According to [30], ERA20 data quality is negatively affected especially in regions of sparse coverage such as the Southern Hemisphere by changes in the observing system, so it shows better agreement in the Northern Hemisphere. ERA20 has been used recently in the study of wave and coastal evolution along the last century over regions like the

Niger Delta [31] and Bay of Bengal [32], or in the global study of the evolution of extreme wave heights and its connection with climate variability [33].

- ERA-Interim (henceforth ERAI) [34]. This is a global reanalysis from 1979, which is continuously updated every month. The data assimilation method is 12-h 4D-Var and is based on a 2006 release of the IFS (Cy31r2). The wave model is based on the Wave Modeling Project (WAM) approach [35], and includes shallow-water physics [36]. Additionally, the new version of WAM has reduced the RMSE in the wave period against buoy data compared to ERA40's error [37]. The spatial resolution is approximately 75 km (ERA20 is almost two times coarser) and wave parameters can be obtained 6-hourly.

For the validation against measurement buoys 6-hourly data have been used in the intersection period between ERA20, ERAI and buoys. In contrast, monthly mean values, obtained from the daily mean values, have been used for the posterior calibration and trend evaluation. The spatial resolution recommended by ECMWF has been used in the two reanalysis.

2.1.2. Buoy data

Fig. 1 presents the area of study and the four buoys chosen from the resources offered by the Spanish Port Authority [24]. The area of study is a slightly wider than the Bay of Biscay, also including the buoy in front of Galicia (Cabo Silleiro), in Gascogne (GS) and in Brittany (BT), provided by the MetOffice UK. Hence the two reanalysis and the calibrated model can be studied also in open ocean, far from the coast. Finally, another one near-shore buoy within the Bay has also been used: Bilbao-Vizcaya (BV).

Table 1 presents the geographical positions of the buoys and the distance of the nearest ERA20 gridpoint where the validations against the buoy's wave observations have been calculated. The last column presents the validation period of the reanalysis and the calibrated dataset against the buoys.

2.2. Methodology

2.2.1. Empirical quantile-matching calibration

In previous studies in the literature, different calibration or bias correction techniques have been developed and compared analyzing climatological parameters, such as temperature and precipitation (see Refs. [38–40]). These methods are usually designed to compare model and reanalysis results with observations, or results from different models at different spatial and temporal scales. In the present paper, a simple but effective statistical procedure based on distribution mapping is used to show the validation process over the buoys within the area of study (see Fig. 6). The idea of distribution mapping is to correct the distribution function of the model's values to fit values of a better model or the observed distribution function. The mapping can be achieved generating a transfer function to map the occurrence distributions. For this approach, several other names can be found in the literature, mainly for precipitation and temperature, such as 'probability mapping' [41], 'quantile-quantile mapping' [42,43], 'statistical downscaling' [44] and 'histogram equalization' [45].

Table 1
Buoys on the bay of Biscay.

Buoy, abbreviation	Position (lon,lat)	Nearest gridpoint	Validation Period
1. Brittany, BT	(-8.47, 47.55)	51.9 km	1998–2010
2. Cabo Silleiro, CS	(-9.43, 42.12)	65.5 km	1998–2010
3. Gascogne, GC	(-5.00, 45.23)	46.8 km	1998–2010
4. Bilbao-Vizcaya, BV	(-3.05, 43.64)	36.9 km	1991–2010

Within this general approach, empirical quantile-mapping bias correction has been applied to calibrate ERA20 versus ERAI [46]. In Ref. [47] the same procedure is developed for wind speed bias correction between ERA20 and ERAI, and to the best knowledge of the authors, it is one of the first studies about the implications of climate trends on renewable energies (wind industry in this case). This method of calibration or bias correction is fundamentally statistical and the idea is to match the values with the same quantile after obtaining two empirical probability distributions: the one that will be calibrated (ERA20) and the one that is the basis for the calibration (ERAI). In Fig. 2, arrows illustrate the interpolation in the quantile-matching procedure to convert the wave energy from the original ERA20 data to their calibrated counterparts establishing the same quantile value in the cumulative distribution functions (CDF) curves of ERA20 and ERAI. These CDF curves correspond to the BV buoy's nearest gridpoint, a wave energy value from the ERA20 before calibration (*bc*) is transformed to its higher counterpart at the same level in the cERA20 distribution after calibration (*ac*), which coincides with the ERAI curve. As a preliminary result, we also show the buoy's CDF, which is between ERA20 and ERAI curve, but, as expected, closer to the ERAI curve.

2.2.2. Wave energy flux and wave periods

Significant wave height (H_s, in meters) and mean wave period (T_m, in seconds) are the relevant wave parameters in the ERAI and ERA20 reanalysis, because they are the provide the wave energy flux (WEF) in kW/m:

$$WEF = 0.49 * H_s^2 * T_m; \tag{1}$$

where H_s and T_m are obtained from the wave spectral moments as shown in Eqs (2)–(4):

$$H_s = 4\sqrt{m_0} \tag{2}$$

$$T_m = m_{-1}/m_0, \tag{3}$$

and the spectral moments are given by

$$m_n = \int_0^\infty \omega^n S(\omega) d\omega, n = -1, 0, 1, 2\ldots \tag{4}$$

where ω is the wave frequency and $S(\omega)$ the wave spectrum.

However, the typical periods available in buoy measurements

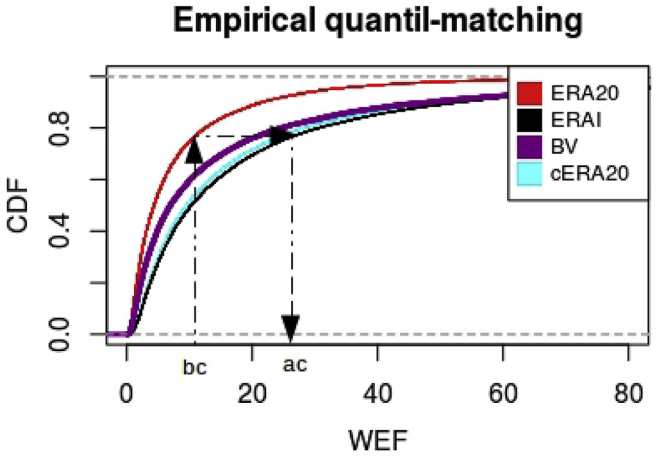

Fig. 2. Illustrating quantile-matching calibration for wave every over CDF curves.

are the average zero-crossing period ($T_z = sqrt(m_0/m_2)$) and the peak period (T_p). This is also the case in the buoys used in this paper. Consequently, considering different spectra (JONSWAP, Bretschneider, etc), wave period ratio (WPR) is usually defined as T_m/T_z in order to relate these different periods and to correct the WEF equation according to T_z . Previous studies, such as [48] have shown that $WPR = 1.12$ is appropriate in general, reaching up to 1.33 in extreme cases like Ireland (Loop Head). In any case, the WRF is just a scale-factor and, therefore, is irrelevant for the final trend computation. However, in ERA20 and ERAI wave field's, the peak period parameter is also available, so there is no need to adapt the average zero-crossing period.

Therefore, the correction of WEF based on the WPR has been only used for the validation between the models and in situ buoy observations, as shown in Section 2.2.3. ERA20 and ERAI wave datasets also offer the parameter called *wave period based on the second moment*, that is, T_z, with which a WPR of approximately 1.3 has been found to give the best results for the four buoys, showing a reasonably low variability (a relative standard error of 2–3%).

2.2.3. Representation of correlation, RMSE and SD ratio

The validation of the two reanalysis and the calibration process has been made versus the observations provided by the four buoys. Three statistical indicators are represented by Taylor Diagrams:

- Root Mean Square Error (RMSE), represented by the arcs with the centre in the observation point;
- Pearson correlation coefficient, represented by the exterior arc;
- and the ratio of standard deviations between the model and the observation (SDratio), represented by the interior arc in case of SDratio = 1.

Hence, the positions of ERA20, ERAI, and the calibrated cERA20 are shown in the diagrams. Each evaluation point is extended by a cloud of points, the contour of which represents the confidence level of 95% generated via bootstrap resampling with 1000 samples. Such contour permits to identify whether the differences in the validation of ERA20, ERAI and cERA20 are statistically significant.

In addition, ERA20 versus ERAI correlation and bias maps are used for Europe in order to study the similarity between the two reanalysis. This could be important to obtain a preliminary idea about a possible over/under estimation of the wave energy flux by ERA20 or other kind of differences in the intersection period of 32 years with ERAI (1979–2010).

2.2.4. Trend maps

Trend maps are drawn over the Bay of Biscay calibrating ERA20 at each gridpoint against ERAI's nearest gridpoint wave data series. Furthermore, European maps are also shown to have a more general idea about the differences apportioned by the calibration to the trends with respect to pure ERA20 trends and in order to compare them with global ship observations [7] and satellite altimeter data [12]. The trends have been calculated using Theil-Sen [49,50] method and their significance has been assessed at a 95% confidence level using bootstrap resampling. Monthly data is used and previously historical monthly averages are subtracted from the series to take into account monthly anomalies. In every case, the trend per decade is shown.

In addition, the trends corresponding to the zonal and meridional components of wave power have also been drawn to see which direction is predominant in the historical increase or decrement of wave power.

2.2.5. PDF evolution and the implementation of WEC's power matrix

In order to calculate the power matrix of WECs, the PDF matrices for the do-decades of the 20th century are given as a function of significant wave height (H_s) and peak period (T_p), showing the evolution of the PDF matrices with respect to the first do-decade throughout the 20th century. Fig. 9 shows the absolute PDF of the first do-decade above, and the differential PDFs of the next four do-decades with respect to the first one below. This way of representation allows us to visualize the evolution of the PDFs along time and to see if the probability of energetic events (higher H_s and higher T_p) is increasing or decreasing.

This method introduces a new perspective connected with the energy production of WECs by means of the wave height-period sea-state determination at a given location and the implementation of the WEC's power matrix. Therefore, it does not consider the orientation of the shore with respect to the wave energy flux direction as in the most modern estimations on wave energy resource assessment [14].

The power matrix illustrates an estimate of the power that a specific WEC can absorb from ocean waves at a specific location. Such power matrix is determined, in this case, by means of a frequency-domain linear hydrodynamic model, similarly to [3,51], assuming the fluid is non-viscid and incompressible, the flow is irrotational and the amplitude of the motions are sufficiently small compared to the wavelength and the device dimensions. The equation of motion of the WEC in frequency-domain is given as follows,

$$(M + A_{rad}(\omega))\ddot{X} + (B_{rad}(\omega) + B_{PTO})\dot{X} + K_H X = \widehat{F}_{exc} \tag{5}$$

where M is the mass of the device, $A_{rad}(\omega)$ and $B_{rad}(\omega)$ are the radiation added-mass and damping, respectively, X is the position of the body, K_H the hydrostatic stiffness, B_{PTO} the damping coefficient of the power take-off (PTO) force and $\widehat{F}_{exc} = \Re(Fe(\omega)e^{i\omega t})$ the excitation force vector per unit of wave amplitude that includes the incident and diffracted wave fields. Frequency-domain hydrodynamic coefficients $A_{rad}(\omega)$, $B_{rad}(\omega)$, K_H and $F_{exc}(\omega)$ are calculated using the open-source boundary element method solver NEMOH [52].

A spherical heaving point absorber (PA) of 5 m of diameter, based on the WAVESTAR device [53], is selected to examine the impact of the PDF evolution in the performance of a WEC, when deployed in the Bay of Biscay. Fig. 3 schematically illustrates the selected WEC and the PTO system.

Such PTO system is modeled as a linear damper, for which the damping coefficient is optimized for each sea-state using the brute force strategy, i.e. iterative simulation with a maximum-search algorithm, ensuring that the global maximum was always reached. Fig. 4 illustrates the power matrix of the selected WEC with the optimal PTO damping coefficient.

To determine the power matrix, average power absorption of the WEC at each sea-state (assuming irregular waves) must be evaluated. First, absorbed power per unit of wave amplitude is calculated in regular waves as follows,

$$P_r(\omega) = \frac{1}{2} B_{PTO}\omega^2|\delta|^2 \tag{6}$$

where δ is the device motion amplitude normalized against the wave amplitude. Power absorbed in regular waves is then used, in combination with a wave energy spectrum ($S(\omega)$) associated to a specific sea-state, to obtain the mean absorbed power at each sea-state as follows,

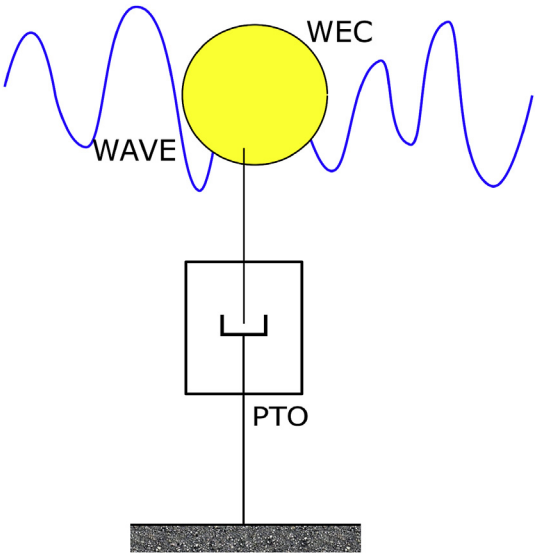

Fig. 3. Schematic view of the wave energy converter and the power take-off device.

$$P_{SS}(H_s, T_p) = \int_0^\infty P_r(\omega) S(\omega) d\omega \tag{7}$$

The energy density spectrum of each sea-state is given, in this paper, by the well-known JONSWAP spectrum [54]. Fig. 4 illustrates the power matrix obtained for the spherical PA employed in this study.

The combination of the power matrix and the PDF matrix, as described in Equation (8), provides the annual mean power production (AMPP) of a WEC at a given location. The annual energy production (AEP) can be obtained straight away multiplying the AMPP by the number of hours in a year.

$$AMPP = \sum_{i=1}^{N_H} \sum_{j=1}^{N_T} P_{SS}(H_s(i), T_p(j)) PDF(H_s(i), T_p(j)) \tag{8}$$

where N_H and N_T are, respectively, the number of significant wave heights and peak periods included in the PDF matrix.

3. Results

3.1. Similarity maps and Taylor Diagrams

Fig. 5 presents the WEF's bias and correlation of ERA20 versus ERAI over Europe in order to get a general idea of their similarity. The correlation is optimal over the Atlantic Ocean and very good over the Mediterranean sea, with losses that happen only near-shore. However, the bias map shows a general overestimation of ERA20 with respect to ERAI in the Atlantic, mainly in the West of Ireland, and a weaker underestimation over the Mediterranean. Therefore, the calibration of ERA20 against ERAI cannot improve the correlation, but it may achieve improvements in the correction of the error (the root mean square error or the standard deviation ratio). That is what Taylor Diagrams represent.

Taylor Diagrams for the four buoys illustrated in Fig. 6 show important improvements due to calibration. In every case the calibrated ERA20, referred to as cERA20, approaches ERAI considerably, which always is closer to observation than ERA20. Taking into account the cloud of points that define the contour for 95% confidence level, ERA20, ERAI and cERA20 show the same correlation value for all the cases, meaning that the calibration cannot improve the correlation. However, significant improvements in RMSE appear in all the cases except in GC, bringing the calibrated data's RMSE from 20 to 25 kW/m to 10–15 kW/m. The approach of cERA20 to the arc that defines the SD ratio 1 is also considerable in the four cases.

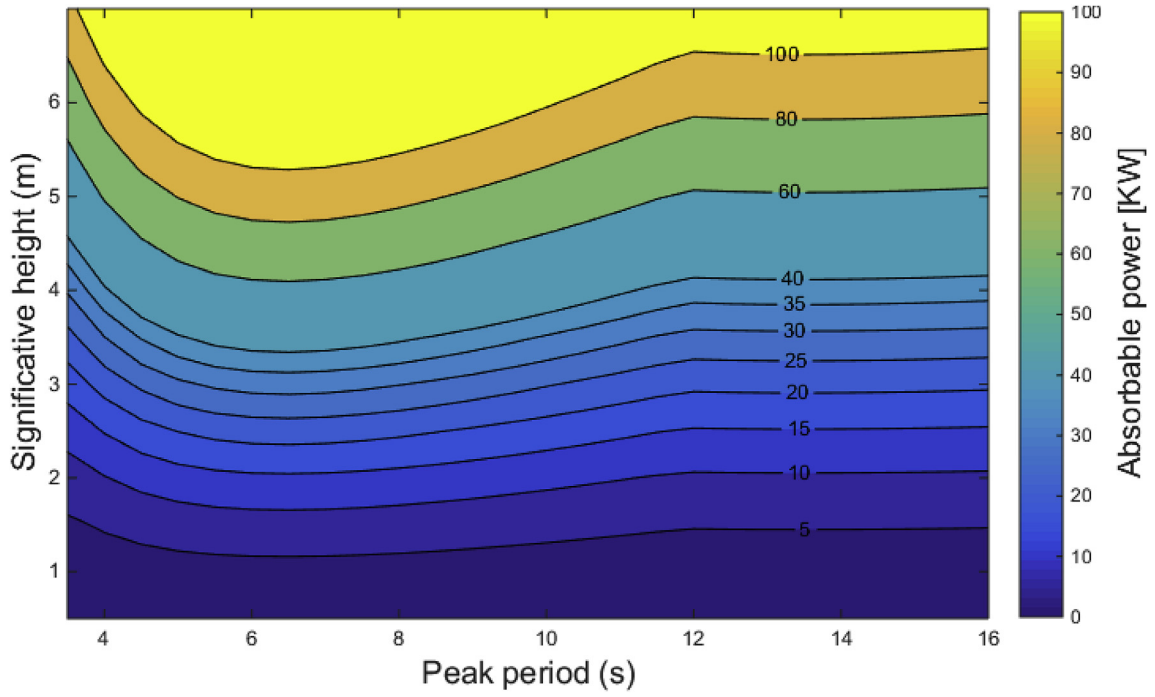

Fig. 4. Power matrix of the spherical heaving point absorber.

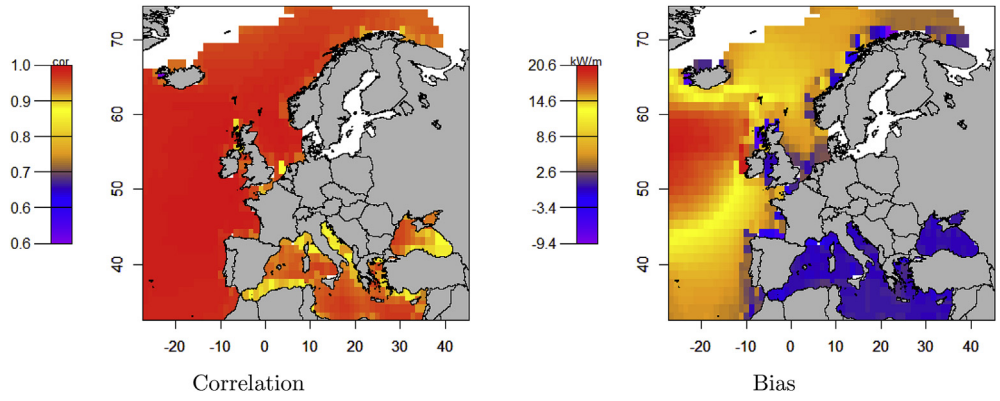

Fig. 5. WEF's bias and correlation of ERA20 versus ERAI over Europe.

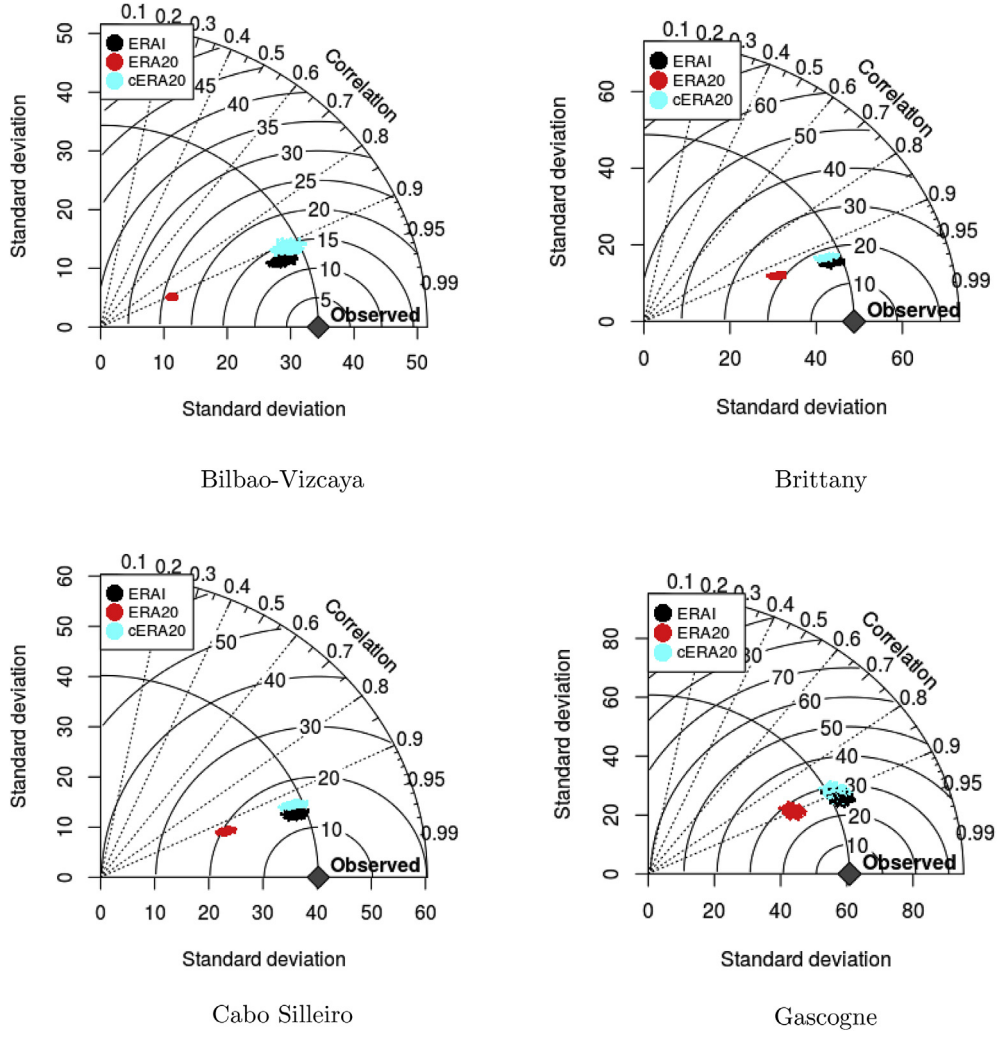

Fig. 6. Taylor Diagrams of ERA20, ERAI and cERA20 in the four buoys.

3.2. Wave energy trend maps

Given the satisfactory validation results of the ERA20 versus ERAI calibration in the buoys, a first WEF's trend map for Europe is presented in Fig. 7 to achieve a more general spatial understanding about the influence of calibration on wave energy trends. Fig. 7 illustrates the trends according to pure ERA20 on the left, with a hot area over the West of Ireland that reaches increments of wave power till 1.1 kW/m per decade. Moreover, the calibrated cERA20, shown in the map on the right in Fig. 7, gives even higher values, with differences of 0.5 kW/m in the mentioned hot area (figure on the right). Therefore we can say that the wave power trend is between 1.1 and 1.6 kW/m per decade in this extreme location and that the underestimation of WEF trends in ERA20 is general all over

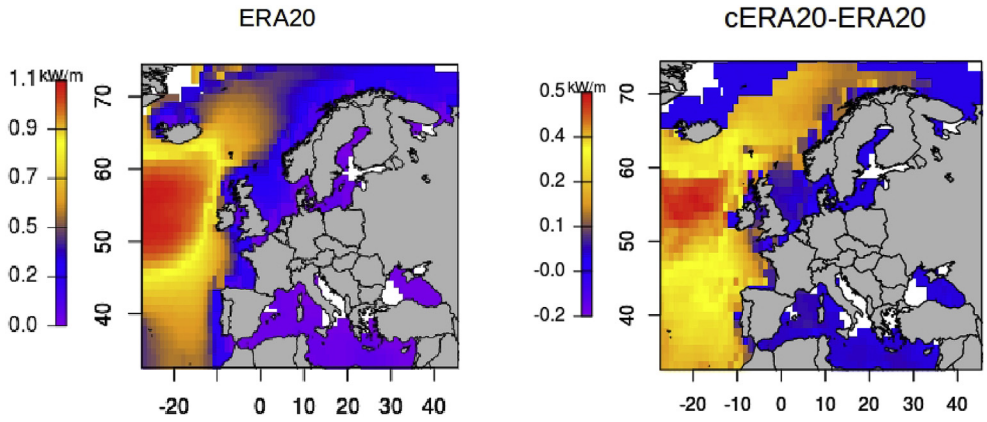

Fig. 7. Wave energy trend in Europe according to ERA20 and the difference by calibration.

Europe, mainly in the open Atlantic Ocean.

Henceforth using the new calibrated ERA20 data set, Fig. 8 shows the decadal trends of H_s, T_m, WEF, and the zonal and meridional components of WEF for the Bay of Biscay. All the trends are positive and increase towards the Atlantic open sea, except wave period, which presents a curious pattern in the interior of the Bay with increments of 6.5 cs per decade and with a general increment over the area of study. Wave height presents an increment of 5 cm per decade in the Northwest of Galicia (half a meter along all the century), and therefore, wave power reaches trends above 1 kW/m in this region. The zonal and meridional trends present respectively similar increments from the West and from the North, which supposes a coherent pattern given that the predominant wind and wave direction of our study area is from Northwest.

3.3. Results for a generic wave energy converter

The H_s and T_p two-variable PDFs for the do-decades of the last century show important consequences for WECs. The referential PDF around the Bilbao-Vizcaya buoy of the first do-decade is on the top of Fig. 9 and the following four do-decades are represented below shown as differential PDFs with respect the first one. The displacement of the positive colors towards higher wave heights

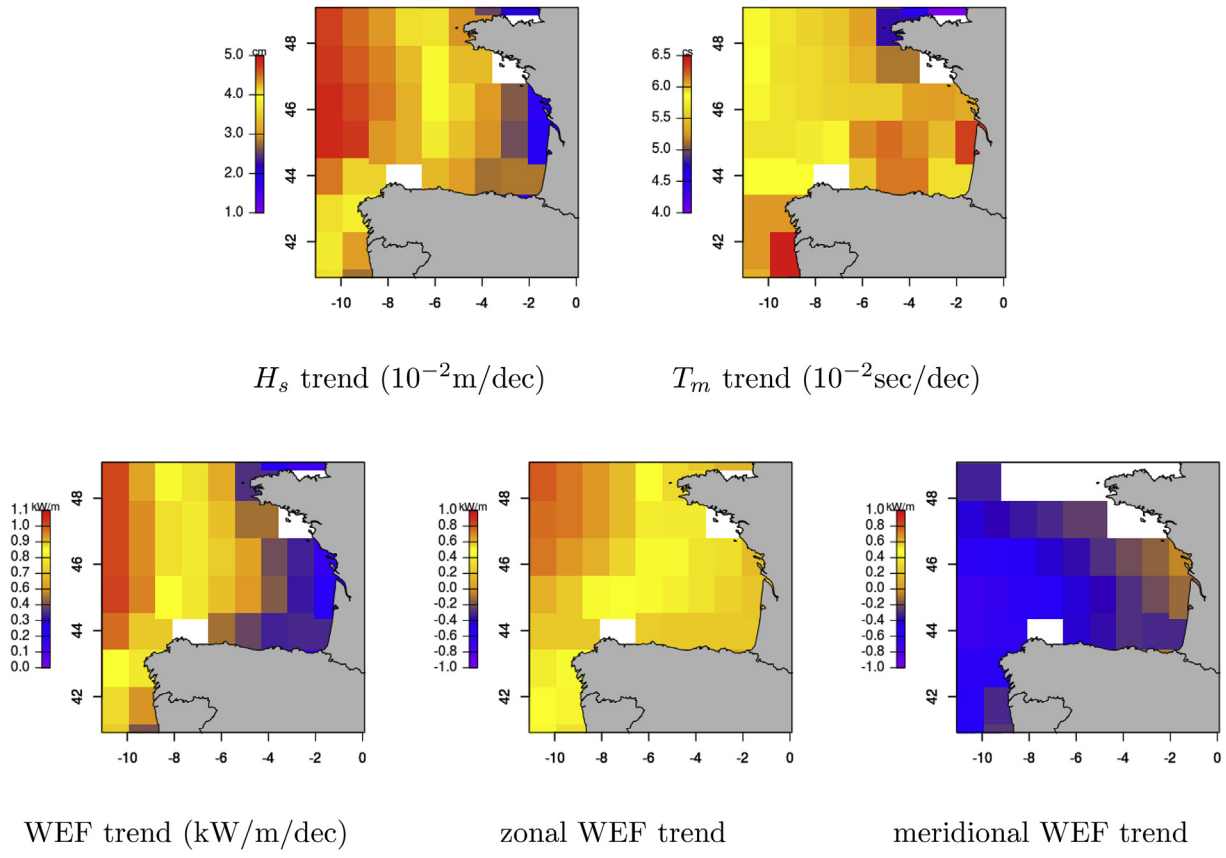

Fig. 8. Trends over the bay of Biscay.

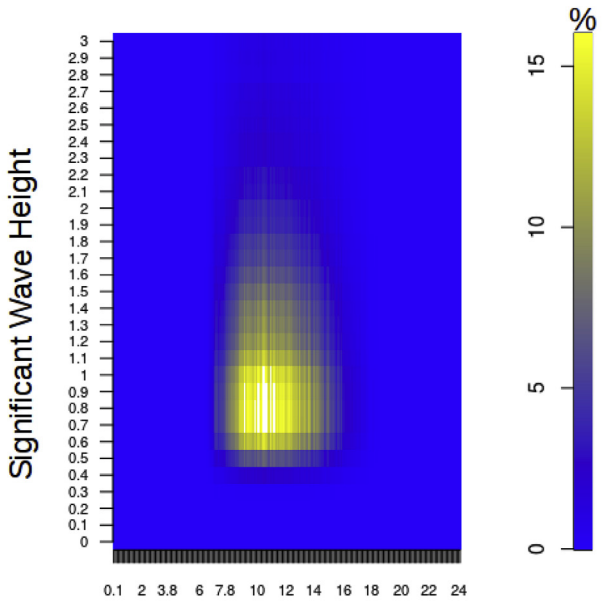

1900-20 PDF

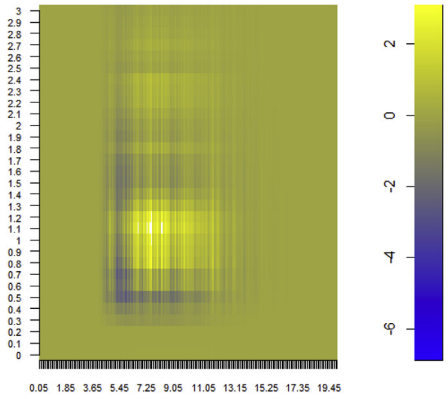

1920-40 differential PDF

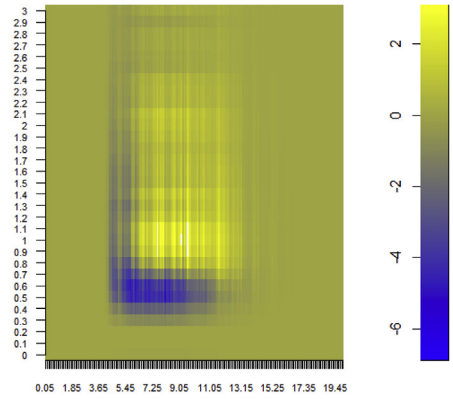

1940-60 differential PDF

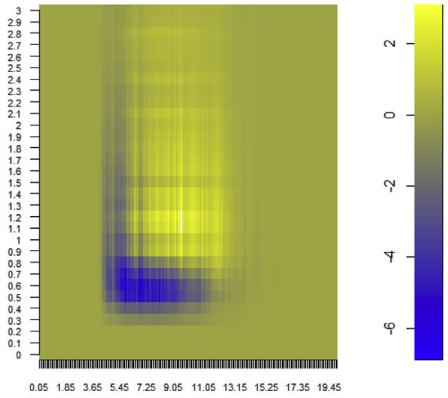

1960-80 differential PDF

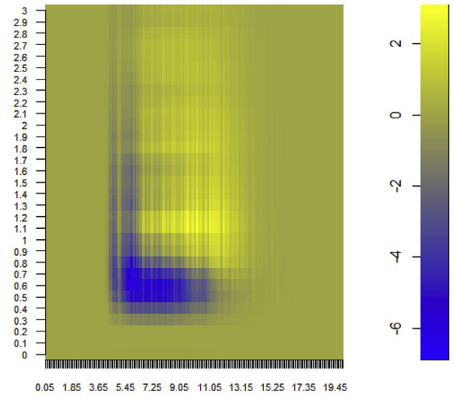

1980-2000 differential PDF

Fig. 9. On the top, the absolute PDF of the first do-decade, and below the differential PDFs of the next four do-decades with respect to the first one.

and wave periods is clear along the time. So the probability of low energetic events diminishes and the probability of high energetic events increases. In addition, this displacement is progressive along the do-decades, mainly along the last three ones (from 1940 to 2000), with an important leap in the 40s.

This historical displacement towards more energetic sea events presents clear consequences for wave energy production. For the above mentioned generic device, Table 2 shows the evolution along the do-decades of averages of sea parameters like H_s, T_m, T_p and wave energy production parameters like AMPP and AEP together with the respective perceptual increase compared with average of the first do-decade. We find total increments between the first and last do-decades of 15% for mean H_s (from 1.57 m to 1.80 m) and of 7% for mean T_m and T_p. Implementing the power matrix of our device, this implies a total AEP and AMPP increment along the century of more than 30%; for example, there is a very significant increment of almost 10% between the last two do-decades going from a mean AEP of 112 MWh to 120 MWh.

Table 2: H_s, T_p and WEF mean values for each do-decade, and the AMPP and AEP by the considered generic device near the Bilbao-Vizcaya buoy.

Means	1900–1920	1920–1940	1940–1960	1960–1980	1980–2000
H_s (m)	1.57	1.58	1.64	1.74	1.80
H_s (+%)	–	0	4	11	15
T_m (sec)	8.20	8.28	8.54	8.64	8.75
T_p (sec)	9.92	10.01	10.33	10.45	10.57
T_p, T_m (+%)	–	1	4	5	7
AMPP (kW)	10.48	10.60	11.21	12.83	13.75
AMPP (+%)	–	0	7	22	32
AEP (MWh)	91.8	92.8	98.2	112.3	120.5
AEP (+%)	–	1	7	22	31

4. Discussion

In a previous study [55], authors found that, in some cases, WAM poorly captures the land-sea boundaries and the local bathymetry close to shore. As a result, in some locations WAM does not represent accurately H_s, T_p and, subsequently, WEF. However, in other locations like the ones shown here (BV and CS buoys) WAM accurately represents buoy observations. In this near-shore locations, and also in open sea, trends are solid and clearly indicate a general increase of WEF in the last century.

None of the previous studies on wave trends have considered variations of the wave period, mainly focusing on wave height. Therefore, trends of WEF cannot be accurately studied, since WEF is proportional to wave period and this paper has demonstrated that wave period significantly varies along the 20th century. Peak period increased by 7% in the last do-decade with respect to the first one, which contributes to the wave power increment. This is a significant contribution compared with a wave power estimation made only using wave heights. In any case, the present paper is a preliminary study and the exact value of these demonstrated positive trends must be carefully considered, since, for example, satellite altimeter data assimilation has shown that reanalysis (Japan JRA-55 in this case) overestimates wave energy flux trends [56].

However, we must note that these results are totally consistent with the above mentioned studies by Young et al. [12], who have calculated wave height positive trend between 0 and 5 cm per decade (0.25% per year considering 2 m mean H_s) from satellite altimeter data in our area of study over an approximate period of two decades. Bertin's work [16] based on ERA20 also shows very similar results over the Bay of Biscay, as expected. It is also consistent with Gulev's work with ship data [7] where the observed trend is also very similar: 4–6 cm/decade in the interior of the Bay with an increment towards the open ocean in the Northwest. Furthermore, it should be noted that our spatial resolution is three or four times finer than the previous studies in the literature.

The above mentioned increase towards the open ocean is expectable because the swell waves are generated in open ocean and loose energy as they approach the coast. The comparison presented in Ref. [12] between the global wind speed trends and wave height trends shows this aspect in the middle of the Atlantic Ocean, where wind blows for a duration of time over a fetch of water generating the swell. Generally speaking, the contribution of the swell is more important than local wind waves and therefore the WEF is mainly dominated by the swell.

This is connected with the similar contribution of zonal and meridional components to WEF in Fig. 8. The positive values (from the West) in the zonal component reaches almost 1 kW/m a value similar but opposite to the negative values (from the North) in the meridional component. It is well known that the predominant wind and swell wave direction over the Bay of Biscay is from the North-West, where the main swell generation area in the middle of the North Atlantic is located [15,57].

Regarding the technological aspect, an operating lifespan of 20–30 years is considered, in general, for wave energy devices [58,59]. Hence, a wave energy plant, including aspects like moorings lines, PTO system and power transmission cables, must be designed to absorb power from and survive to ocean waves throughout the whole lifespan. Commonly, the wave energy plant is designed based on the wave resource characteristics of the past years, optimizing the plant for those characteristics. However, this paper demonstrates that wave resource characteristics varied significantly in the past century, with substantial variations within a period of time equivalent to the lifespan of the wave energy plant, up to a 16% increase in the WEF in 20 years as shown in Table 2. As a consequence, a wave energy plant that is designed using only the resource characteristics previous to the deployment date may waste a significant part of future waves' energy or fail to survive the unpredicted extreme wave conditions.

5. Conclusions and future outlook

The main conclusions of this study can be resumed like this:

1. According to ERA20's last century data and its calibration against ERAI over the Bay of Biscay there is a historical spatial average positive trend of 0.7 kW/m/decade in WEF and of 4 cm/decade in wave height.
2. For the considered WEC in a near-shore position the energy production along the century would increase significantly, more than 30% since 1900.
3. In the last do-decade, when our reanalysis data are more reliable due to a higher number of assimilated data, the increment in energy production would be almost 10%.
4. The displacement along the century towards more energetic events of the wave height-period PDF necessitates taking into account this evolution for the pre-design of WEC.

According to the do-decade analysis around the location of the BV buoy, it should be considered, apart from the historical positive trend, the leap in wave height, wave period and consequently in WEF produced in the 1940s. This kind of observations may be an initial point for a further study between the relation of the global climate change and global wave energy trends. The key question would be to understand the cause of this positive trend in order to determine whether this trend will remain so in the future.

The major meteorological centers carry out reanalysis in order to avoid as much as possible the inhomogeneities in the climate

record due to the changes in the operational weather forecast models which affect the quality of meteorological archives. In order to achieve this goal, these centers use frozen data assimilation systems to avoid the impact of changes in the numerical models in the long-term climatic variability that is saved into meteorological archives. However, previous studies [60] have already shown that the temporal variations in the amount of information that can be assimilated due to the development with time of meteorological observing networks makes sometimes impossible to completely avoid the inhomogeneities in the record. The observing networks have evolved with time both in number of stations reporting to the meteorological centers but also in the kind of observations made available, with the introduction of satellite soundings after 1979 marking a qualitative and quantitative change in the amount of available information. Recent studies [61] have shown that for the case of ERAI, this problem is not very important and it can produce a credible estimate of temperature at several layers of the atmosphere, since this reanalysis was started together with the major improvements of the meteorological observing system. This might not be the case for ERA20C reanalysis, which extends longer back in time than ERAI and could, therefore, be more seriously affected. The trends in extra-tropical cyclones and windstorms in ERA20C and NOAA-20CR reanalysis were studied by Ref. [62]. They found significant differences in the trends of cyclones and windstorms in both reanalysis, particularly during early periods of the 20th Century. Both reanalysis agree better in terms of extreme cyclones, but, still, some differences exist. Currently, the direct comparison between our results with the ones from NOAA's 20th Centruy RA is not possible, since no a wave model is included in the reanalysis from NOAA. However, further research should be carried out in the existence of spurious trends in the ones that have been presented in this paper due to the changing amount of surface observations available for assimilation with time.

Since the historical in-situ information is the one that has been assimilated for the most part (exception made of some isolated buoys in some countries), and since observational records for our area do not extend much back in time, it is probably wiser to perform analysis by comparing the distribution of wave parameters in climate-change like models, such as the one used in Ref. [63]. Under this setup, the evolution of wave statistics can be studied as a result of the external forcing alone, without any impact of the trends in the amount of available observations. However, for this type of studies other problems would arise, such as the effect of the model biases in quantile-quantile matching technique and its applicability under climate-change scenarios. Therefore, this is still an area of open research and it is outside the scope of this paper.

Although combined wind and swell waves have been considered in this work, the trends of wind waves and swell waves can also be studied separately in the future. A further refinement can be also obtained with the new reanalysis of ECMWF calibrating CERA-20C [64] against ERA5 [65].

With respect to WECs, mooring lines and PTO systems are, in general, designed for individual WECs, for which results shown in this paper address the main challenges arose due to resource variations. In contrast, aspects like power transmission lines are rather designed for WEC arrays where tens or hundreds of devices are deployed.

Indeed, variations in the wave resource are expected to have a greater impact in WEC arrays than in individual devices, since an increase of 15% in AMPP results in an increment of less than 2 kW for a single device, as shown in Table 2, but an increment of about 200 kW for an array of 100 WECs. However, to accurately evaluate the impact of resource variations in power transmission lines, WEC arrays should be considered in the hydrodynamic model presented in Section 2.2.5, since hydrodynamic interactions among the WECs in the array can strongly affect the power output of large arrays, as shown in Ref. [66]. In addition, the WEC selected in this paper is a rather small WEC with relatively low power output, which suggests that the impact of resource variations may be more relevant for larger devices.

The evolution of the wave resource characteristics is only studied in the Bay of Biscay, where the wave resource is moderate compared to other locations in the world, such as Ireland, Chile, South Africa or Australia [67], and so variations in the wave resource should also be studied in these more powerful locations. A well informed decision making process regarding these long-term changes must necessarily include some sort of wave climate forecasting [68].

Future works will focus on evaluating the impact of resource variations in WEC arrays and WECs of different characteristics at locations with different resource characteristics. Additionally, the implications of the sum of WEF increment and sea-level rise should be also studied in the future not only over the WECs but also over the coastal infrastructures constructed at the beginning of the 20th century.

Acknowledgments

This work has been funded bu the Spanish Government MINECO Project CGL2016-76561-R (MINECO/EU ERDF), the University of the Basque Country (projects GIU14/03 and PES17/23). Most of the calculations and plots have been carried out within the framework of R [69]. The authors want to express their gratitude to Puertos del Estado (Spain) and MetOffice (UK) for providing buoy data for this study. The authors with the Centre for Ocean Energy Research are supported by the Science Foundation Ireland under Grant No. 13/IA/1886.

References

[1] Torre-Enciso Y, Ortubia I, de Aguileta LL, Marqués J. Mutriku wave power plant: from the thinking out to the reality. In: Proceedings of the 8th european wave and tidal energy conference, Uppsala, Sweden, vol. 710; 2009.
[2] Nielsen K, Pontes T. Generic and site related wave data. 2010. Final technical report T02–1.1, OES-IEA.
[3] Babarit A. Impact of long separating distances on the energy production of two interacting wave energy converters. Ocean Eng 2010;37(89):718–29. https://doi.org/10.1016/j.oceaneng.2010.02.002.
[4] W. M. Organization. Calculation of monthly and annual 30-year standard normals. 1989. WCDP-No. 10. WMO-TD/No. 341., Tech. rep.
[5] W. M. Organization. The role of climatological normals in a changing climate. 2007. WCDMP-61, WMO-TD/1377, Tech. rep.
[6] Ruggiero P, Komar PD, Allan JC. Increasing wave heights and extreme value projections: the wave climate of the US Pacific Northwest. Coast Eng 2010;57(5):539–52.
[7] S. K. Gulev, V. Grigorieva, Last century changes in ocean wind wave height from global visual wave data, Geophys Res Lett, 31(24).
[8] Gulev SK, Grigorieva V. Variability of the winter wind waves and swell in the North Atlantic and North Pacific as revealed by the voluntary observing ship data. J Clim 2006;19(21):5667–85.
[9] Gulev SK, Cotton D, Sterl A. Intercomparison of the North Atlantic wave climatology from voluntary observing ships, satellite data and modelling. Phys Chem Earth 1998;23(5):587–92.
[10] Bouws E, Jannink D, Komen G. The increasing wave height in the North Atlantic Ocean. Bull Am Meteorol Soc 1996;77(10):2275–7.
[11] D. K. Woolf, P. Challenor, P. Cotton, Variability and predictability of the North Atlantic wave climate, J Geophys Res Oceans, 107 (C10).
[12] Young I, Zieger S, Babanin AV. Global trends in wind speed and wave height. Science 2011;332(6028):451–5.
[13] Zheng CW, Wang Q, Li CY. An overview of medium- to long-term predictions of global wave energy resources. Renew Sustain Energy Rev 2017;79:1492–502. https://doi.org/10.1016/j.rser.2017.05.109.
[14] Reguero B, Losada I, Mndez F. A global wave power resource and its seasonal, interannual and long-term variability. Appl Energy 2015;148:366–80. https://doi.org/10.1016/j.apenergy.2015.03.114.
[15] Zheng C, Shao L, Shi W, Su Q, Lin G, Li X, et al. An assessment of global ocean wave energy resources over the last 45 a. Acta Oceanol Sin 2014;33(1):92–101. https://doi.org/10.1007/s13131-014-0418-5.
[16] Bertin X, Prouteau E, Letetrel C. A significant increase in wave height in the

north atlantic ocean over the 20th century. Glob Planet Change 2013;106:77–83. https://doi.org/10.1016/j.gloplacha.2013.03.009.
[17] Wang XL, Swail VR. Climate change signal and uncertainty in projections of ocean wave heights. Clim Dyn 2006;26(2–3):109–26.
[18] Cox AT, Swail VR. A global wave hindcast over the period 1958-1997- validation and climate assessment. J Geophys Res 2001;106(C2):2313–29.
[19] Sterl A, Komen G, Cotton P. Fifteen years of global wave hindcasts using winds from the European Centre for Medium-Range Weather Forecasts reanalysis: validating the reanalyzed winds and assessing the wave climate. J Geophys Res Oceans 1998;103(C3):5477–92.
[20] Wang XL, Zwiers FW, Swail VR. North Atlantic ocean wave climate change scenarios for the twenty-first century. J Clim 2004;17(12):2368–83.
[21] Kushnir Y, Cardone V, Greenwood J, Cane M. The recent increase in North Atlantic wave heights. J Clim 1997;10(8):2107–13.
[22] Vikebø F, Furevik T, Furnes G, Kvamstø NG, Reistad M. Wave height variations in the North sea and on the Norwegian continental shelf, 1881–1999. Cont Shelf Res 2003;23(3):251–63.
[23] Le Traon PY. From satellite altimetry to argo and operational oceanography: three revolutions in oceanography. Ocean Sci 2013;9(5):901–15. https://doi.org/10.5194/os-9-901-2013.
[24] P.P.E., Puertos del Estado: Oceanography: forecast, real time and climate, Spanish Government: Madrid. Updated 2015-10-11. http://www.puertos.es/en-us/oceanografia/Pages/portus.aspx.
[25] P. Camus, I. Losada, C. Izaguirre, A. Espejo, M. Menéndez, J. Pérez, Statistical wave climate projections for coastal impact assessments, Earth's Future.
[26] Patra A, Bhaskaran PK. Temporal variability in wind–wave climate and its validation with esso-niot wave atlas for the head bay of bengal. Clim Dyn 2016:1–18.
[27] S. Caires, A. Sterl, C. Gommenginger, Global ocean mean wave period data: validation and description, J Geophys Res Oceans, 110 (C2).
[28] Poli P, Hersbach H, Dee DP, Berrisford P, Simmons AJ, Vitart F, et al. ERA-20C: an atmospheric reanalysis of the twentieth century. J Clim 2016;29(11):4083–97.
[29] Worley SJ, Woodruff SD, Reynolds RW, Lubker SJ, Lott N. ICOADS release 2.1 data and products. Int J Climatol 2005;25(7):823–42.
[30] Poli Paul. Natl Cent Atmos Res Staff 2016. 2016-01-19, https://climatedataguide.ucar.edu/climate-data/era-20c-ecmwfs-atmospheric-reanalysis-20th-century-and-comparisons-noaas-20cr.
[31] Dada OA, Li G, Qiao L, Ma Y, Ding D, Xu J, et al. Response of waves and coastline evolution to climate variability off the Niger Delta coast during the past 110 years. J Mar Syst 2016;160:64–80. https://doi.org/10.1016/j.jmarsys.2016.04.005.
[32] Patra A, Bhaskaran PK. Temporal variability in wind–wave climate and its validation with ESSO-NIOT wave atlas for the head Bay of Bengal. Clim Dyn 2016:1–18.
[33] Kumar P, Min S-K, Weller E, Lee H, Wang XL. Influence of climate variability on extreme ocean surface wave heights assessed from ERA-interim and ERA-20C. J Clim 2016;29(11):4031–46. https://doi.org/10.1175/JCLI-D-15-0580.1.
[34] P. Berrisford, D. Dee, K. Fielding, M. Fuentes, P. Kallberg, S. Kobayashi, S. Uppala, The ERA-interim archive.
[35] Komen GJ, Cavaleri L, Donelan M, Hasselmann K, Hasselmann S, Janssen P. Dynamics and modelling of ocean waves. Camb Univ press 1996.
[36] P. Janssen, J.-R. Bidlot, S. Abdalla, H. Hersbach, Progress in ocean wave forecasting at ECMWF, ECMWF Technical Memory 27.
[37] J. Bidlot, P. Janssen, S. Abdalla, H. Hersbach, A revised formulation of ocean wave dissipation and its model impact.
[38] Teutschbein C, Seibert J. Bias correction of regional climate model simulations for hydrological climate-change impact studies: review and evaluation of different methods. J Hydrol 2012;456:12–29.
[39] S. Watanabe, S. Kanae, S. Seto, P. J.-F. Yeh, Y. Hirabayashi, T. Oki, Intercomparison of bias-correction methods for monthly temperature and precipitation simulated by multiple climate models, J Geophys Res Atmos, 117 (D23).
[40] Lafon T, Dadson S, Buys G, Prudhomme C. Bias correction of daily precipitation simulated by a regional climate model: a comparison of methods. Int J Climatol 2013;33(6):1367–81.
[41] Block P, Souza Filho F, Sun L, Kwon H-H. A streamflow forecasting framework using multiple climate and hydrological models,. J Am Water Resour Assoc 2009;45(4):828–43. https://doi.org/10.1111/j.1752-1688.2009.00327.x. cited By 45.
[42] Bo J, Terray L, Habets F, Martin E. Statistical and dynamical downscaling of the seine basin climate for hydro-meteorological studies. Int J Climatol 2007;27(12):1643–55. https://doi.org/10.1002/joc.1602. cited By 128.
[43] Sun F, Roderick ML, Lim WH, Farquhar GD. Hydroclimatic projections for the murray-darling basin based on an ensemble derived from intergovernmental panel on climate change AR4 climate models. Water Resour Res 2011;47(12). https://doi.org/10.1029/2010WR009829. n/a–n/a, w00G02.
[44] Piani C, Haerter JO, Coppola E. Statistical bias correction for daily precipitation in regional climate models over Europe. Theor Appl Climatol 2010;99(1):187–92. https://doi.org/10.1007/s00704-009-0134-9.
[45] Rojas R, Feyen L, Dosio A, Bavera D. Improving pan-European hydrological simulation of extreme events through statistical bias correction of RCM-driven climate simulations. Hydrol Earth Syst Sci 2011;15(8):2599–620. https://doi.org/10.5194/hess-15-2599-2011. cited By 45.
[46] Panofsky H, Brier G. Some applications of statistics to meteorology (Pennsylvania state university, Pennsylvania. 1958. Google Scholar 244.
[47] Bett PE, Thornton HE, Clark RT. Using the Twentieth Century Reanalysis to assess climate variability for the European wind industry. Theor Appl Climatol 2015:1–20. https://doi.org/10.1007/s00704-015-1591-y.
[48] Cahill B, Lewis T. Wave period ratios and the calculation of wave power. In: 2nd marine energy technology symposium METS2014, seattle, wash; 2014.
[49] Sen PK. Estimates of the regression coefficient based on Kendall's tau. J Am Stat Assoc 1968;63(324):1379–89.
[50] Theil H. A rank-invariant method of linear and polynomial regression analysis, 3; confidence regions for the parameters of polynomial regression equations. 1950. p. 1–16. Stichting Mathematisch Centrum. Statistische Afdeling (SP 5a/50/R).
[51] Ricci P, Saulnier J-B, Falcão A. Point-absorber arrays: a configuration study off the Portuguese west-coast. In: Proceedings of 7th european wave and tidal energy conference, porto, Portugal; September, 2007. p. 11–3.
[52] Penalba M, Kelly T, Ringwood JV. Using nemoh for modelling wave energy converters: a comparative study with wamit. In: Accepted in Proceedings of European wave and tidal energy conference, Cork; 2017.
[53] M. Kramer, F. Ferri, A. Zurkinden, E. Vidal, J. P. Kofoed, Experimental validation of numerical models for wave energy absorbers, Struct Des Wave Energy Devices.
[54] Hasselmann K, Barnett T, Bouws E, Carlson H, Cartwright D, Enke K, et al. Measurements of wind-wave growth and swell decay during the joint north sea wave project (JONSWAP). Tech. rep. Hamburg: Deutsches Hydrographisches Institut; 1973.
[55] Ibarra-Berastegi G, Sáenz J, Esnaola G, Ezcurra A, Ulazia A, Rojo N, et al. Wave energy forecasting at three coastal buoys in the bay of Biscay. IEEE J Ocean Eng 2016;41(4):923–9.
[56] Sasaki W. Impact of satellite data assimilation in atmospheric reanalysis on the marine wind and wave climate. J Clim 2016;29(17):6351–61. https://doi.org/10.1175/JCLI-D-16-0056.1. arXiv:https://doi.org/10.1175/JCLI-D-16-0056.1.
[57] NOAA. WAVEWATCH III 2009 national weather service (NWS). National Oceanic and Atmospheric Administration; 2009. http://polar.ncep.noaa.gov/waves/wavewatch/wavewatch.shtml.
[58] Energy O. Cost of energy and cost reduction oppotuinties. Tech. rep. SI Ocean. Strategic Initiative for ocean energy; May 2013.
[59] Astariz S, Iglesias G. The economics of wave energy: a review,. Renew Sustain Energy Rev 2015;45:397–408. https://doi.org/10.1016/j.rser.2015.01.061.
[60] Bengtsson L, Hagemann S, Hodges KL. Can climate trends be calculated from reanalysis data? J Geophys Res 2004;109. https://doi.org/10.1029/2004JD004536. D11111.
[61] Simmons AJ, Poli P, Dee DP, Berrisford P, Hersbach H, Kobayashi S, et al. Estimating low-frequency variability and trends in atmospheric temperature using ERA-Interim. Quart J Roy Met. Soc 2014;140:329–53. https://doi.org/10.1002/qj.2317.
[62] Befort DJ, Wild S, Kruschke T, Ulbrich U, Leckebusch GC. Different long-term trends of extra-tropical cyclones and windstorms in ERA-20C and NOAA-20CR reanalyses. Atmos Sci Let 2016;17:586–95. https://doi.org/10.1002/asl.694.
[63] Dobrynin M, Murawsky J, Yang S. Evolution of the global wind wave climate in CMIP5 experiments. Geophys Res Lett 2012;39(18). https://doi.org/10.1029/2012GL052843. n/a–n/a, l18606.
[64] European Centre for medium-range weather forecasts. 2017. 2017-06-01, https://www.ecmwf.int/en/research/climate-reanalysis/cera-20c.
[65] European Centre for medium-range weather forecasts. 2017. 2017-06-01, https://www.ecmwf.int/en/newsletter/147/news/era5-reanalysis-production.
[66] M. Penalba, I. Touzon, J. Lopez-Mendia, V. Nava, A numerical study on the hydrodynamic impact of device slenderness and array size in wave energy farms in realistic wave climates, Submitted to Ocean Engineering.
[67] Mork G, Barstow S, Kabuth A, Pontes MT. Assessing the global wave energy potential. In: ASME 2010 29th international conference on ocean, offshore and Arctic engineering. American Society of Mechanical Engineers; 2010. p. 447–54.
[68] Lpez-Ruiz A, Bergillos RJ, Ortega-Snchez M. The importance of wave climate forecasting on the decision-making process for nearshore wave energy exploitation. Appl Energy 2016;182:191–203. https://doi.org/10.1016/j.apenergy.2016.08.088.
[69] Core Team R. R: a language and environment for statistical computing. R Foundation for Statistical Computing; 2016. https://www.R-project.org.